An Analysis of Fuel Cell Options for an All-Electric Unmanned Aerial Vehicle

Lisa L. Kohout
Glenn Research Center, Cleveland, Ohio

Paul C. Schmitz
Power Computing Solutions, Inc., Avon, Ohio

NASA STI Program . . . in Profile

Since its founding, NASA has been dedicated to the advancement of aeronautics and space science. The NASA Scientific and Technical Information (STI) program plays a key part in helping NASA maintain this important role.

The NASA STI Program operates under the auspices of the Agency Chief Information Officer. It collects, organizes, provides for archiving, and disseminates NASA's STI. The NASA STI program provides access to the NASA Aeronautics and Space Database and its public interface, the NASA Technical Reports Server, thus providing one of the largest collections of aeronautical and space science STI in the world. Results are published in both non-NASA channels and by NASA in the NASA STI Report Series, which includes the following report types:

- TECHNICAL PUBLICATION. Reports of completed research or a major significant phase of research that present the results of NASA programs and include extensive data or theoretical analysis. Includes compilations of significant scientific and technical data and information deemed to be of continuing reference value. NASA counterpart of peer-reviewed formal professional papers but has less stringent limitations on manuscript length and extent of graphic presentations.

- TECHNICAL MEMORANDUM. Scientific and technical findings that are preliminary or of specialized interest, e.g., quick release reports, working papers, and bibliographies that contain minimal annotation. Does not contain extensive analysis.

- CONTRACTOR REPORT. Scientific and technical findings by NASA-sponsored contractors and grantees.

- CONFERENCE PUBLICATION. Collected papers from scientific and technical conferences, symposia, seminars, or other meetings sponsored or cosponsored by NASA.

- SPECIAL PUBLICATION. Scientific, technical, or historical information from NASA programs, projects, and missions, often concerned with subjects having substantial public interest.

- TECHNICAL TRANSLATION. English-language translations of foreign scientific and technical material pertinent to NASA's mission.

Specialized services also include creating custom thesauri, building customized databases, organizing and publishing research results.

For more information about the NASA STI program, see the following:

- Access the NASA STI program home page at *http://www.sti.nasa.gov*

- E-mail your question via the Internet to *help@sti.nasa.gov*

- Fax your question to the NASA STI Help Desk at 301–621–0134

- Telephone the NASA STI Help Desk at 301–621–0390

- Write to:
  NASA Center for AeroSpace Information (CASI)
  7115 Standard Drive
  Hanover, MD 21076–1320
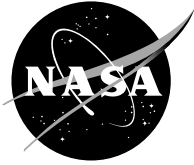
An Analysis of Fuel Cell Options for an All-Electric Unmanned Aerial Vehicle

Lisa L. Kohout
Glenn Research Center, Cleveland, Ohio

Paul C. Schmitz
Power Computing Solutions, Inc., Avon, Ohio

National Aeronautics and
Space Administration

Glenn Research Center
Cleveland, Ohio 44135

May 2007

An Analysis of Fuel Cell Options for an
All-Electric Unmanned Aerial Vehicle

Lisa L. Kohout
National Aeronautics and Space Administration
Glenn Research Center
Cleveland, Ohio 44135

Paul C. Schmitz
Power Computing Solutions, Inc.
Avon, Ohio 44011

Abstract

A study was conducted to assess the performance characteristics of both PEM and SOFC-based fuel cell systems for an all-electric high altitude, long endurance Unmanned Aerial Vehicle (UAV). Primary and hybrid systems were considered. Fuel options include methane, hydrogen, and jet fuel. Excel-based models were used to calculate component mass as a function of power level and mission duration. Total system mass and stored volume as a function of mission duration for an aircraft operating at 65 kft altitude were determined and compared.

Introduction

A study was performed at the NASA Glenn Research Center to evaluate concepts for fuel cell-based propulsion systems for all-electric high altitude, long endurance Unmanned Aerial Vehicle (UAV) applications. Fuel cells exhibit a higher efficiency than combustion engines, and therefore may enhance or enable long endurance UAV missions. When operated on hydrogen, the byproducts of the fuel cell reaction are heat and water. Although large quantities of heat can be generated during operation, in many instances the heat can be recaptured and supplied to other processes, such as heating of reactants or fuel processing, or the hot exit streams can be expanded in a turbine to produce power. As part of this effort, system studies were conducted to identify concepts with high payoff potential and associated technology areas for further development. Areas under consideration included: proton exchange membrane (PEM) and solid oxide fuel cells (SOFC); primary, regenerative, and hybrid systems; hydrogen, methanol, methane, and jet fuels; and gaseous, cryogenic, and liquid fuel storage. This paper details the results of an analysis performed on a set of fuel cell system architectures for a UAV operating at 65 kft altitude.

The two main fuel cell types under consideration for aircraft applications are the PEM and the SOFC. Each of these systems offers distinct advantages as well as issues associated with their use in aircraft propulsion applications. PEM fuel cell technology is at a relatively high state of development due to major investments in recent years by the automotive industry. PEM fuel cells operate at relatively low temperatures (20 to 90 °C) and use a proton-conducting polymer membrane as an electrolyte. The anode and cathode are catalyzed porous electrodes bonded directly onto the membrane to form a single cell called a membrane electrode assembly (MEA). Cells are connected electrically in series with bipolar plates, which also serve to deliver and distribute the fuel and oxidant to the anode and cathode. For the most part, PEM fuel cells use hydrogen as the fuel, although some small direct methanol systems have been developed in which the methanol is directly reduced to carbon dioxide and water within the fuel cell. Because PEM systems operate below the temperate necessary for reformation, a separate reformer is needed if hydrocarbon-based fuels are used. In addition, PEM fuel cells are highly sensitive to sulfur and CO in the reformate stream and both must be eliminated by further processing before the stream enters the fuel cell stack.

The solid oxide fuel cell is a ceramic, high-temperature (600 to 1000 °C), solid-state device that uses an oxide ion-conducting ceramic material as the electrolyte. The ceramic anode, electrolyte, and cathode materials are deposited in layers to form the solid oxide equivalent of the PEM MEA. There are two primary design types, tubular and planar. The tubular design was pioneered by the US Westinghouse Electric Corporation (now Siemens-Westinghouse) in the late 1970s and has been used primarily for stationary terrestrial powerplant applications. The more recent planar design resembles the PEM configuration in that the ceramic cells are stacked together in a bipolar configuration using interconnects between the cells to provide a series connection and flow distribution, much like the PEM bipolar plate. The main advantage of the planar design over the tubular is that higher power densities can be achieved due to the lower losses inherent in the bipolar configuration. This is significant for mobile applications where mass and volume are typically limited. The planar design is, however, at a low level of technology development as compared to either PEM or the tubular SOFC. Among the technology challenges that are currently being addressed in the industry are the thermal robustness of the ceramics, cell sealing at high temperatures, and cell scale-up.

Although less technically mature, SOFCs offer some potential advantages over PEM fuel cells for aircraft applications. The SOFC is cooled by flowing excess air through the cathode. This is in contrast to the PEM system where a liquid is pumped through cooling channels within the fuel cell stack and sent to a radiator. By using this high temperature waste heat for other processes in the system, the SOFC can achieve an overall higher system efficiency than PEM, despite its lower Gibbs free energy. The waste heat from the SOFC product stream can be extracted and used for fuel heating, reformation, or expansion through a turbine to extract power to run the fuel cell system ancillary equipment. Unlike the PEM, SOFCs have the option to use CO as a fuel as well as hydrogen. Because of this, hydrocarbon fuels can be more readily used with less processing than in the PEM system. Also, with the high operating temperatures, SOFCs have the potential for direct internal reforming of light hydrocarbons. Direct natural gas reformation has been demonstrated in the tubular design and some work has been done in designing planar stacks with internal processing of natural gas. Additionally, SOFCs are more sulfur tolerant than PEM fuel cells, requiring less fuel processing to reduce sulfur levels.[1]

Approach

Table 1 shows the system configurations considered in this study. System configurations were compared based on overall system mass and fuel tank volume for 10, 100, and 1000 kW power levels for missions times ranging from 12 to 96 hr. Given the large trade space for this effort, a flexible modeling environment was needed in which system configurations could be changed with minimal modification to the models.

TABLE 1.—STUDY MATRIX

Configuration reference no.	Fuel cell type	Fuel	Oxidant	Turbine / generator	Notes
1	PEM	H_2 (g)	Air	No / No	Compressor power provided by fuel cell
2		H_2 (l)	Air	No / No	
3		H_2 (l)	O_2 (l)	No / No	
4		H_2 (l)	Air	Yes / No	Compressor power provided by turbine
5		CH_4 (l) reformate	Air	Yes / No	
6		Jet-A reformate	Air	Yes / No	
7	SOFC	CH_4 (l) reformate	Air	Yes / No	Compressor power provided by turbine
8		H_2 (l)	Air	Yes / Yes	Power to load provided by fuel cell and generator
9		CH_4 (l) reformate	Air	Yes / Yes	
10		Jet-A reformate	Air	Yes / Yes	

A series of Excel-based component models were developed to model each system configuration. A PEM fuel cell stack model was developed which calculates stack performance, mass, and volume based on an input power level, I-V curve, and cell characteristics. This model predicts fuel cell performance using either hydrogen fuel or reformate with air or oxygen as the oxidant. A two-dimensional SOFC model was developed to calculate mass, volume, temperature, reactant concentrations, current, and voltage across each cell for a cross-flow geometry based on a specified set of cell material properties. For this study, the anode material was nickel with yittria stabilized zirconia (YSZ), the electrolyte was YSZ, and the cathode was Sr- doped $LaMnO_3$ (LSM) with YSZ.[2] The interconnect was made of $LaCrO_3$-T. As with the PEM fuel cell, this model will accept either hydrogen or reformate as the fuel source. Reformate composition was determined through a chemical kinetics equilibrium model based on the Chemical Equilibrium with Applications (CEA) code developed at NASA Glenn.[3] The model uses steam reformation and calculates the reformate composition based on input temperature, fuel, and carbon-to-water ratio. An integrated thermodynamic system model was developed to track mass and energy flows in the system.

The compressors and turbines were sized using NASA radial compressor and turbine design codes[4,5], CCD and RTD, respectively, and then scaling relationships were developed to integrate with the Excel-based program. Compressor and turbines speeds were matched and, for the compressors, the pressure ratio was divided evenly between each stage. The compressor wheels were made of aluminum, and the turbine wheels were made of titanium. Heat exchangers were sized using the LACEX[6] design code run for 65 kft altitude to determine an overall heat transfer coefficient. This data was used to perform parametric variations with power. Finally, tank models for the storage of gaseous, cryogenic, and liquid fuels were developed to complete the system. The gas storage model used a tank efficiency factor of 710,000 in., which is based upon work that was performed under the NASA ERAST program for the Helios aircraft.[7] The cryogenic storage tank mass and volume models were based on vacuum jacketed spherical tanks using multi-layer insulation.[8] Bladder tanks were scaled based on commercially available JP-8 tanks to store non-cryogenic liquid fuels.[9]

System Configurations

Ten system configurations were considered as part of this study (table 1). A block diagram of the first two configurations is shown in figure 1.
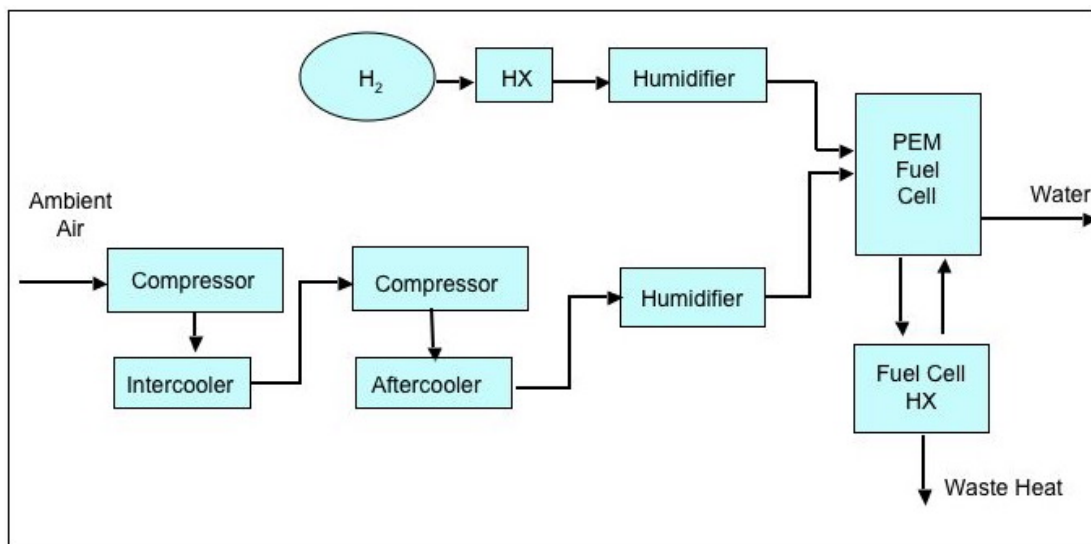

Figure 1.— H2-air PEM fuel cell block diagram.

For these cases, hydrogen in either gaseous or liquid (LH_2) form (configurations 1 and 2, respectively) is fed through a heat exchanger to raise its temperature to the fuel cell operating temperature and is then passed through a humidifier before entering the PEM fuel cell. Humidifiers are required on both the anode and cathode feeds to prevent fuel cell membrane dry-out and maintain conductivity of the membrane. At 65 kft, ambient air enters the first compression stage at 0.8 psi and 216 K. Two stages of compression are used to raise the air pressure to the fuel cell operating pressure of 14.7 psi. The calculated efficiency of the compressors was between 80 and 85%. In order to keep the aluminum compressor wheel within its operating temperature limits, an intercooler removes the heat of compression between stages. Following the second stage of compression, the air is cooled to the fuel cell operating temperature in the aftercooler before entering the humidifier and then the fuel cell. For these configurations, the power required to run the compressors is provided by the fuel cell. Therefore, the fuel cell must be sized to supply both compressor power and payload power. The ratio of gross power output to net power output was determined to be 1.53, which shows the burden that running a compressor levies on the system. A fuel cell heat exchanger is required to remove the fuel cell waste heat via a liquid internal cooling loop that runs through the fuel cell.

A representative H_2-air PEM fuel cell operating curve was chosen.[10] From this curve, the fuel cell operating point of 0.68 V/cell at 1200 ma/cm^2 was chosen to minimize stack size. A fuel cell stack mass per unit active area of 0.3 g/cm^2 was chosen as being representative of a lightweight stack.[11] This fuel cell stack mass was multiplied by total active cell area to determine the overall stack mass. An anode fuel utilization of 100% was chosen to minimize the amount of fuel carried on-board.

Water management within the PEM stack is a significant consideration in any system design. Water management is achieved through a balance between reactant humidification and cathode airflow rate. Too little humidification coupled with large airflows will tend to dry out the membrane. Conversely, too much humidification with slower airflows can lead to cell flooding. In order to achieve adequate water balance in the cells, a cathode utilization of 50% was chosen (i.e. 50% of the oxygen input into the fuel cell is reacted) with 80% anode relative humidity and 50% cathode relative humidity. A summary of the assumptions for H_2-air PEM configuration is given in table 2.

TABLE 2.—ASSUMPTIONS FOR H_2-AIR PEM FUEL CELL SYSTEM

Component	Assumptions
PEM fuel cell	• Utilization: 100% fuel, 50% air • Inlet Relative Humidity: 80% anode, 55% cathode • Operating Point: 0.68V/cell, 1200 mA/cm^2 • Operating Temperature: 80 °C • Operating Pressure: 14.7 psi • Stack mass: 0.3 g/cm^2 • Fuel cell sized to provide compressor power – Ratio of gross power output to net power output = 1.53
Compressors	• Radial compressor - pressure ratio evenly divided between 2 compressors • Intercooler air exit temp set to 540 R; aftercooler air temp set to 635 R • Calculated efficiency of 80 to 85%
Heat exchangers	• Heat exchanger design code LACEX run for 65 kft for Main HX, inter- and aftercoolers to find overall heat transfer coefficient • Overall heat transfer coefficient used for off-design
Tanks	• Gas storage tank efficiency factor of 710,000 in. and 5000 psi for volume calculations • Cryogenic storage tanks are titanium with liners and set for 5% boil off to set insulation thickness

Figure 2 shows the block diagram for the third system configuration. In this system, liquid oxygen (LO_2) replaces the two-stage air compression system. The oxygen is heated via a heat exchanger before passing through the humidifier and fuel cell. The technology assumptions are the same as shown in table 2 for the H_2-air system except that the fuel cell operating curve was adjusted for operation on pure oxygen, which will boost the voltage for a given current density. The operating point chosen for this case was 0.7 V/cell at 1200 mA/cm^2.

The fourth system configuration is shown in figure 3. This configuration uses turbine shaft power to drive the compressors, thus eliminating the need to oversize the fuel cell to provide electrical power to run the compressors. Excess hydrogen is sent through the fuel cell and mixed with the fuel cell exit air stream in a burner to raise the exhaust temperature. The hot exhaust from the burner is then expanded through a turbine located on a common shaft with the compressors. The turbine is assumed to be a radial turbine with a titanium wheel and a calculated efficiency of between 85 and 90%. Although the fuel cell is now sized to provide only load power, some additional hydrogen must be carried to feed to the burner. The fuel cell operating parameters are again the same as in table 2 with the exception that the fuel utilization is now 85% instead of 100%, with the excess fuel being burned to provide the energy to run the turbine.
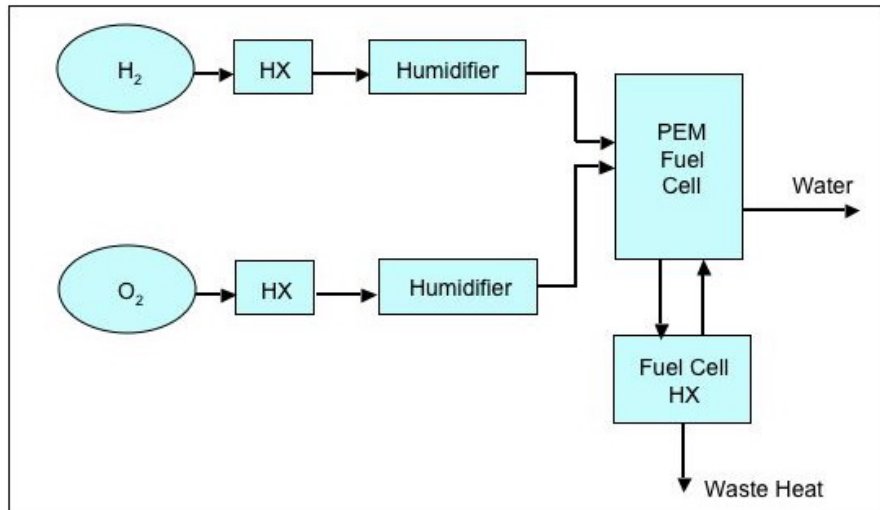
Figure 2.—H_2-O_2 PEM block diagram.
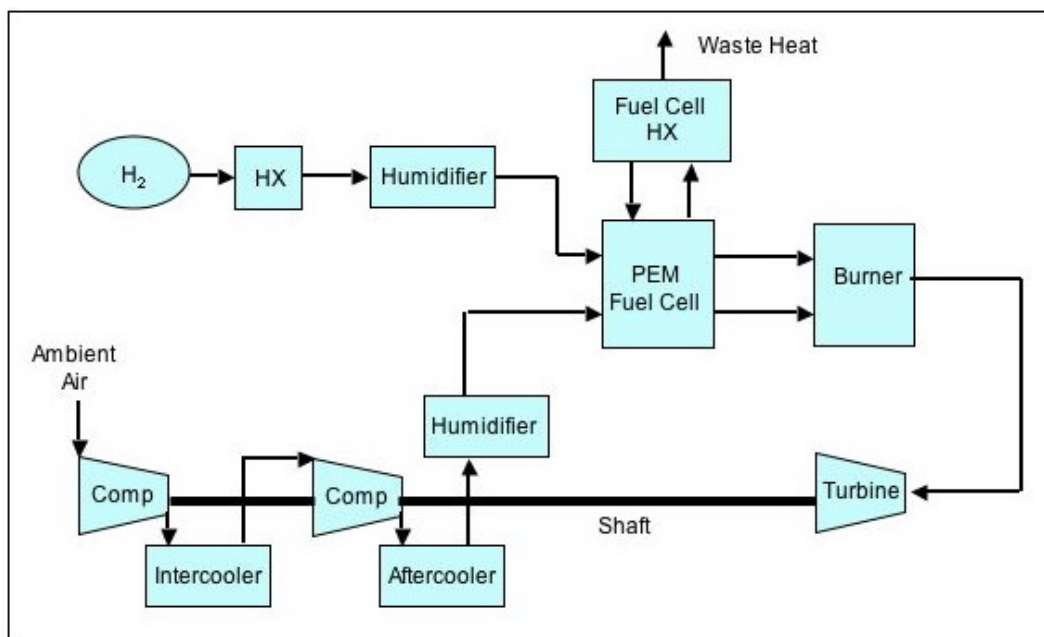
Figure 3.—H_2-air PEM fuel cell with turbine.

Configurations 5, 6, and 7 are depicted in figure 4. This configuration is similar to Configuration 4 except that liquid methane and Jet-A are considered as fuels in place of hydrogen. Configurations 5 and 6 consist of a PEM fuel cell with liquid methane and Jet-A fuel, respectively. Configuration 7 is based on an SOFC with liquid methane. Liquid methane and Jet-A contain more energy per unit volume than hydrogen and can increase mission endurance for a given fuel tank volume. However, when using these fuels with a fuel cell, a reformer must be inserted into the system to convert the fuel into usable hydrogen, which increases system mass. Jet-A was not considered with the SOFC in this configuration since it was anticipated that the greatest benefit of using Jet-A with an SOFC would be realized in the hybrid system to be discussed later.

As is seen in figure 4, the fuel is sent to a reformer where it is broken down into a mixture of 3% hydrogen, 12% carbon monoxide (CO) and 23% carbon dioxide (CO_2) with the remainder comprised of N_2 and H_2O. In addition, a small amount of the fuel is also sent to a burner to provide heat for the reformation reaction. In the case of the SOFC, both the hydrogen and CO are consumed within the stack while the CO_2 passes through the stack as an inert species. In the case of the PEM fuel cell, a CO scrubber is included in the mass of the reformer to alleviate CO poisoning of the membrane electrode assemblies while the CO_2 passes through as an inert species. On the air side, two stages of compression are used as in the previous systems. However, the SOFC system does not require an aftercooler as the heat of compression can be fed directly into the SOFC. A fuel cell HX is included in the PEM cases to reject the waste heat from the stack, while in the case of the SOFC, excess air is moved through the stack to provide cooling. As in the Configuration 4, excess fuel is burned, and the hot exhaust is expanded through the turbine to drive the compressors.

A summary of the assumptions for Configurations 5,6, and 7 is shown in table 3. The PEM voltage was adjusted based on the Nernst equation for operation on reformate. The SOFC operating voltage was determined by the 2-D modeling code previously discussed. The air flow rate was adjusted to maintain a 100K temperature rise across the SOFC stack in order to limit the thermal stress on the materials. Based on the model, the required airflow was calculated to be approximately eight times the flow required to provide sufficient oxygen based on the stoichiometry of the reaction. A fuel utilization of 85% was chosen for the SOFC. It was found that fuel utilizations of about 85% provided adequate energy to run the turbomachinery and, in addition, provide reasonable temperature profiles across the stack.
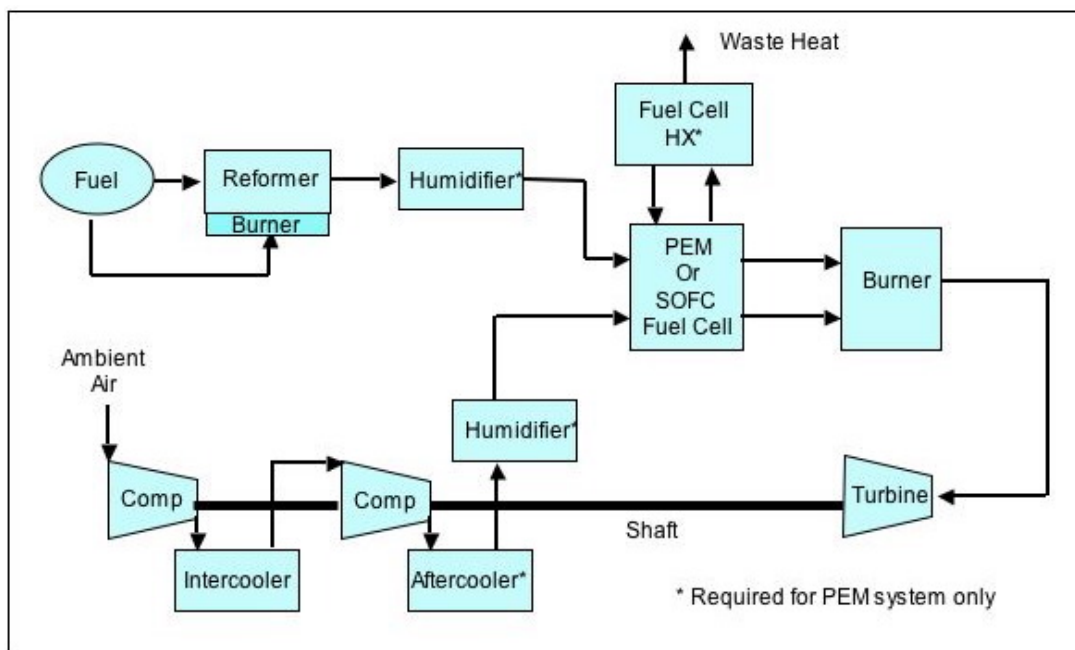

Figure 4.—Block diagram of PEM or SOFC system with turbine and reformed fuel.

TABLE 3.—ASSUMPTIONS FOR PEM OR SOFC SYSTEM WITH TURBINE AND REFORMED FUEL

Component	Assumptions
PEM fuel cell	• Utilization: 85% fuel, 50% air • Inlet Relative Humidity: 80% anode, 55% cathode • Operating Point: ~0.67V/cell, 1200 mA/cm^2 for operation on reformate • Operating Temperature: 80 °C • Operating pressure: 1 bar (14.7 psi) • Stack mass: 0.3 g/cm^2
Solid oxide fuel cell	• 85% fuel utilization, 8X air stoichs • Operating point: 0.7 V/cell, 288 mA/cm2 for CH4 reformate (based on 2-D SOFC model) • Operating Temperature: 1000 K (inlet) • Assume max temp rise across stack of 100 K • Operating Pressure: 3 bar (44 psi) • Stack mass determined from component build-up via SOFC model (~0.8 to 1.0 kW/kg depending on fuel)
Reformer	• Equilibrium conditions assumed at outlet • Concentrations based on CEA code • Steam reformation using 2.5:1 H_2O:C ratio at 1000 K • Assumed mass of 0.5 kg/kW for SOFC systems and 0.75 kg/kW for PEM

Currently, little information is available for lightweight, efficient reformers for methane and Jet-A, making it difficult to estimate the mass of this component. Direct reforming of methane and Jet-A on the anode side of SOFC stacks has been demonstrated, but is still at a low technology readiness level and not considered in this study. PEM systems cannot support direct reforming and require a separate reformer. Additionally, since PEM systems are intolerant to CO, a scrubber must also be included to remove the CO from the reformed fuel before it enters the PEM stack. For the purposes of this study, it was assumed that there was a separate fuel-reforming component for both the PEM and SOFC systems that was composed of material similar to the anode material of a SOFC stack with half the mass of the SOFC stack (anode-only materials). Additional mass was added to the PEM reformation component to allow for CO scrubbing.

The final three configurations considered in this study were SOFC hybrid systems. The block diagram for the SOFC hybrid system is shown in figure 5.
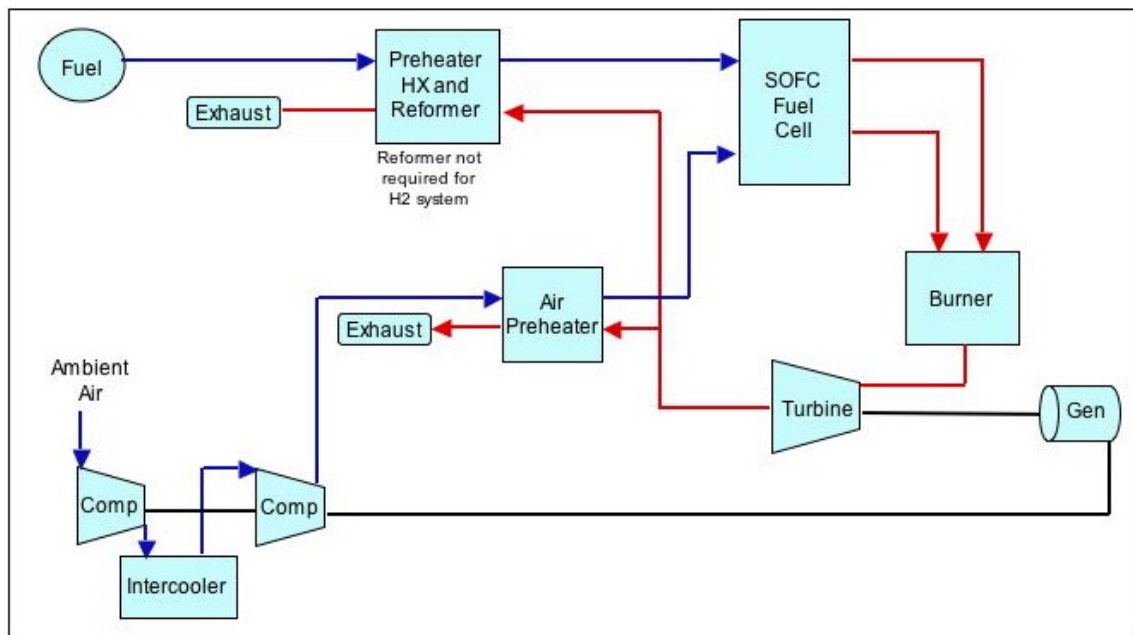
Figure 5.—Block diagram of SOFC hybrid system.

In the hybrid system, the turbine provides shaft power to run the compressors as well as a generator, which produces electrical power. In this system, the aircraft load power is supplied by both the fuel cell and generator. In order to maximize system efficiency, heat exchangers are used to recover exhaust heat and place it back into the system for preheating the incoming air and fuel streams and to provide the heat of reformation.

Referring to table 1, Configuration 8 is an SOFC hybrid system with hydrogen fuel. Configurations 9 and 10 use liquid methane and Jet-A fuel, respectively. The SOFC operating point, based on the 2-D model, was 0.7 V/cell at 288 mA/cm2 for liquid methane and 0.7 V/cell at 268 mA/cm2 for Jet-A. The fuel utilization ranged from 50 to 85% with 8X air stoichs being run through the fuel cell to maintain the 100K delta T across the stack. A bladder tank was used to store the Jet-A fuel. All other assumptions remain the same as for the previous configurations.

Discussion of Results

For each configuration, the total system mass and fuel tank volume was calculated for 10, 100, and 1000 kW net output power for mission times ranging from 12 to 96 hr. Figure 6 shows a plot of the total system mass, including storage tanks, for all of the 10 kW PEM-based configurations considered as a function of mission duration, while figure 7 shows a comparison of tank volume for each of these systems. Tank volume is an important figure of merit when comparing systems for long duration UAV missions since, as mission duration increases, the tanks will begin to dominate the system due to the increased fuel and/or oxidant storage requirement.

As expected, the gaseous storage option results in both the largest system mass and tank volume. The tank volumes for the gaseous H_2-air system have been omitted from figure 7 since the tank volume is nearly 20 times larger than the volume of the LH_2-air system. Comparing the LH_2-air (no turbine) and LH_2-LO_2 systems shows the relative merit of compressing air versus carrying an oxidizer on board. On a mass basis, it is preferable to compress air than carry liquid oxygen. However, when comparing total tank volume, there is a slight advantage for the LO_2 due to the fact that the fuel cell does not need to provide compressor power as well as load power, resulting in a lower specific fuel consumption (0.054 kg/kW-hr for H_2-O_2 system vs. 0.087 kg/kW-hr for LH_2-air) and, therefore, a smaller fuel storage requirement.
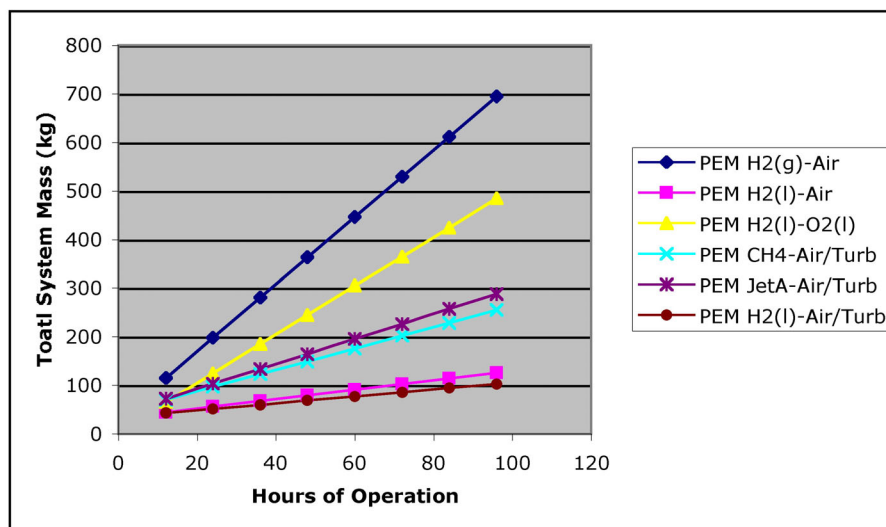
Figure 6.—System mass summary for all PEM systems—10 kW net power output.
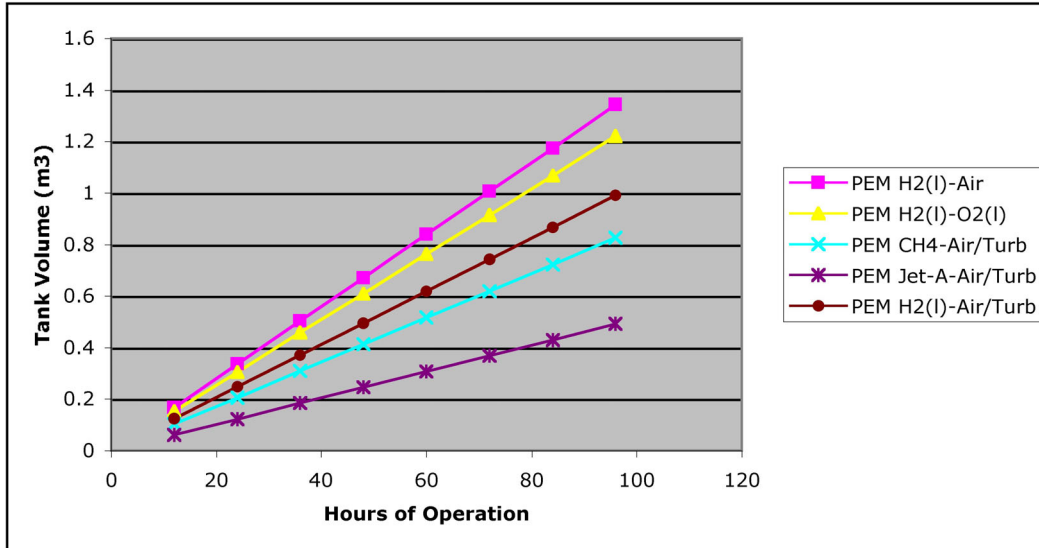
Figure 7.—Tank volume summary for all PEM systems 10 kW net power output.

Another interesting comparison is between the LH$_2$-air systems, with and without a turbine. These systems have similar total masses even though the first system supplies the compressor power via an oversized fuel cell while the latter incorporates the turbine to provide shaft power for compression. The savings in fuel cell and storage tank mass is offset by the increased mass of the turbomachinery. However, the LH$_2$-air/turbine system offers a benefit of smaller tank volume due to lower fuel consumption (0.064 kg/kW-hr with the turbine vs. 0.087 kg/kW-hr without).

Finally, comparing all of the fuel cell systems with turbines shows the relative benefits of the different fuels. The LH$_2$ system has the lowest mass of the three systems, due primarily to the lower total fuel weight and also to the lack of a reformer. However, the benefit of using higher energy density fuels is seen by looking at the plot of tank volume as a function of mission duration. The high density of Jet-A results in the smallest tank volume, showing that for a volume limited UAV, Jet-A may be the best fuel choice. The plots of PEM system mass and tank volume for the 100 and 1000 kW systems follow the same trend as for the 10 kW system and are contained in the Appendix (figs. A1 to A4).

Figure 8 shows a plot of system mass as a function of hours of operation for the 10 kW SOFC-based systems while figure 9 shows the corresponding plot of tank volume.

The main advantage of the high temperature SOFC is that, since the SOFC is air-cooled, it is possible to use the exit product stream to drive a turbine and extract useful work for both powering the compressor and driving a generator. This benefit is illustrated by comparing the methane systems with the turbine only and with the turbine/generator. Off-loading some of the load power generation from the fuel cell to the generator, leads to lower fuel flow rates (0.16 kg/kW-hr with turbine vs. 0.25 kg/kW-hr without) and therefore, lower tank mass and volume. For this study, a 50/50 power split between the fuel cell and generator resulted from the recovery of energy from the unused fuel exiting the stack and the approximately 35% waste heat from the fuel cell. The decrease in fuel cell and compressor mass more than compensates for the increase in turbine/generator mass. In fact, all of the SOFC systems that included the turbine/generator in the configuration had lower mass and volume than the methane system with the turbine only.

Comparing the three SOFC turbine/generator systems operating on different fuels shows the same trends as with the PEM systems with the LH$_2$ system having the lowest mass but the largest tank volume. As with the PEM systems, the plots of SOFC system mass and tank volume for the 100 and 1000 kW systems follow the same trend as for the 10 kW system and are contained in the Appendix (figs. A5 to A8).
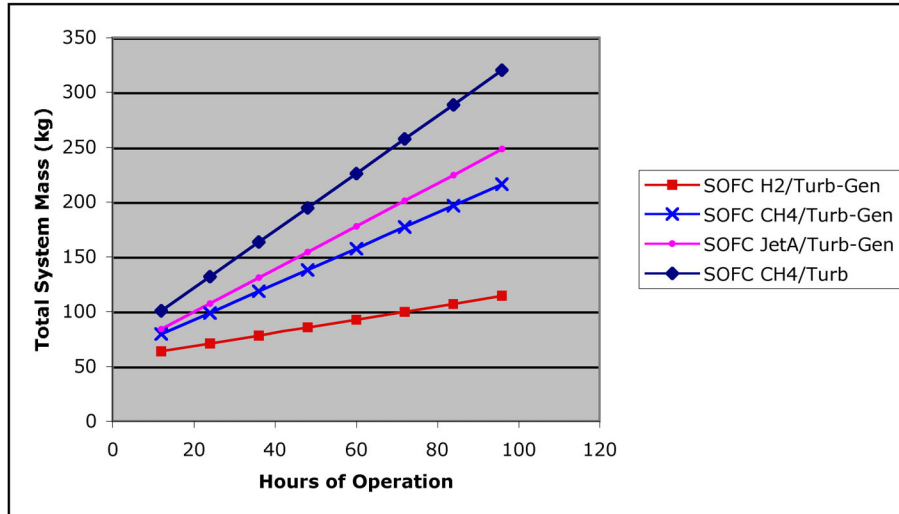
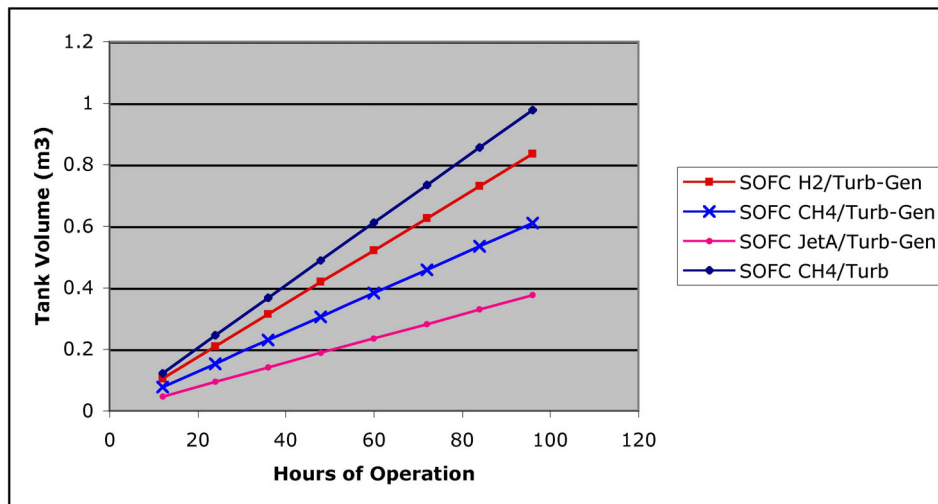Figure 8.—System mass summary for all SOFC systems—10 kW net power output.

Figure 9.—Tank volume summary for SOFC systems—10 kW net power output.

Figure 10 shows the mass breakdowns of various 10 kW PEM and SOFC systems for a 12 hr mission. The three lowest mass systems of each fuel cell technology are represented in this figure. Each of the PEM systems incorporate a turbine (T) to power the fuel cell compressor and are fueled by either liquid hydrogen, liquid methane, or Jet-A. The SOFC systems incorporate both a turbine and generator (T-G), which runs the compressor and also supplies partial power to the payload. As with the PEM systems, the SOFC systems are fueled either by liquid hydrogen, liquid methane, or Jet-A. As can be seen from these figures, the turbomachinery mass dominates for the shorter mission duration. This is especially true for the SOFC systems, which have an additional generator that the PEM systems do not carry. The fuel cell subsystem mass includes the fuel cell and ancillaries as well as the reformer for the methane and Jet-A fuels. The PEM fuel cell mass is heavier than the SOFC mass, in part because the PEM supplies all payload power while the SOFC supplies only about 50% of the power due to the generator. Also, for the methane and Jet-A systems, the reformer mass is heavier to account for the CO removal in the PEM systems, which reflects the assumptions stated in table 3). Despite this mass difference, the PEM systems have less mass in all cases because of the greater turbomachinery mass of the SOFC.
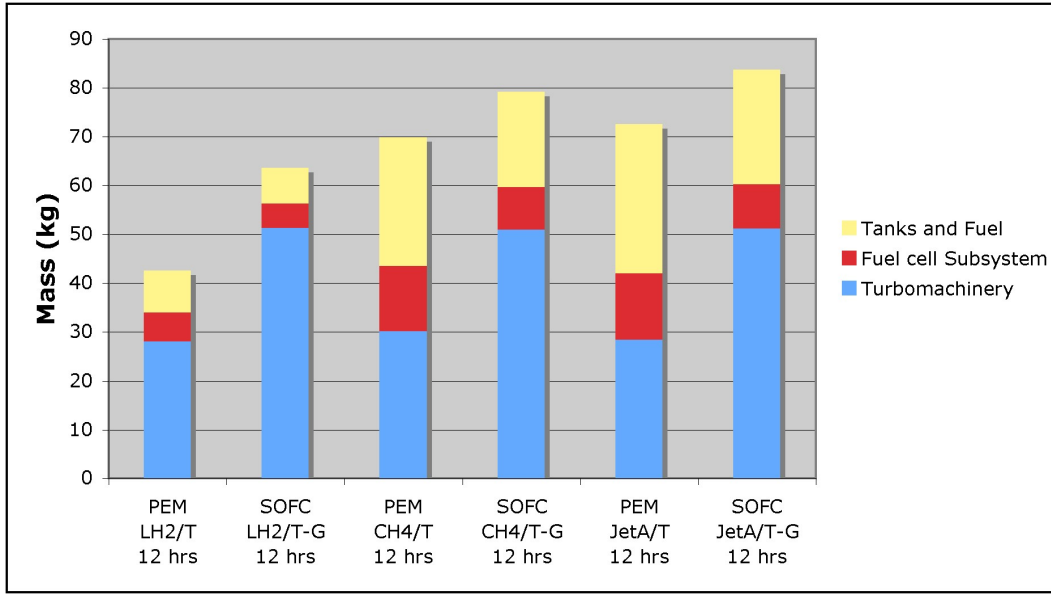
Figure 10.—Mass breakdown for select 10 kW PEM and SOFC systems—12 hr endurance.
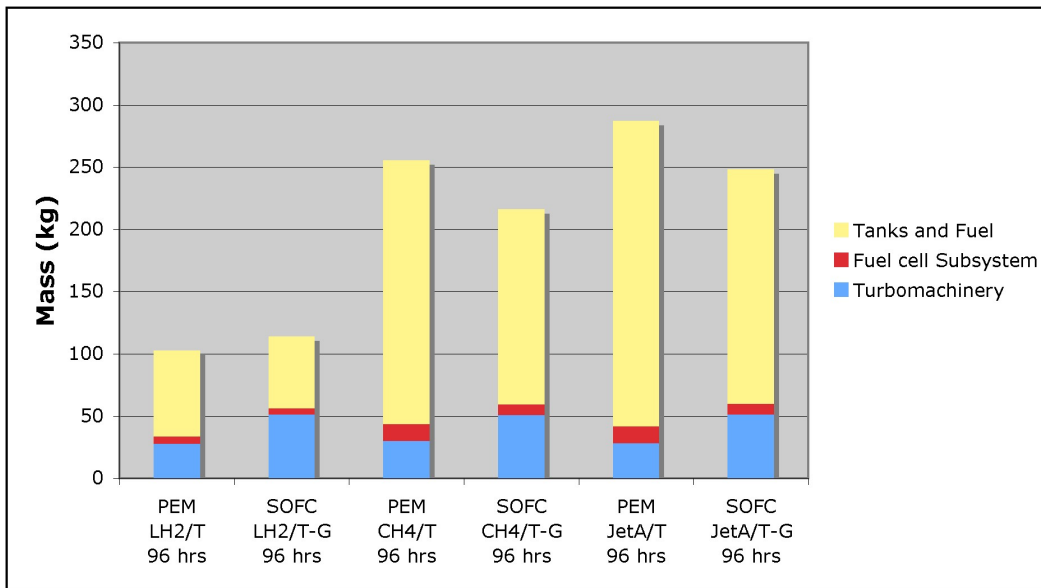
Figure 11.—Mass breakdown for select 10 kW PEM and SOFC systems—96 hr endurance.

As mission length increases, the tank and fuel mass begins to dominate the total system mass (fig. 11). This is more pronounced for the methane and Jet-A systems due to the higher molecular weight of the fuels.

Figures 12 and 13 show corresponding plots for the 1000 kW systems. As the power level increases, the tank mass becomes more dominant, even at 12 hr. It is interesting to note that, unlike the 10 kW systems, the fuel cell subsystem is a greater fraction of the overall mass than the turbomachinery at 12 hr. This is due to the fuel cell subsystem mass scaling linearly with power while the turbomachinery specific mass flow (kg/hr mass flow per kg turbomachinery) increases with increasing throughput, resulting in masses that are less than they would be if scaled linearly. The mass breakdown charts for the 100 kW systems are included in the Appendix (figs. A9 and A10).
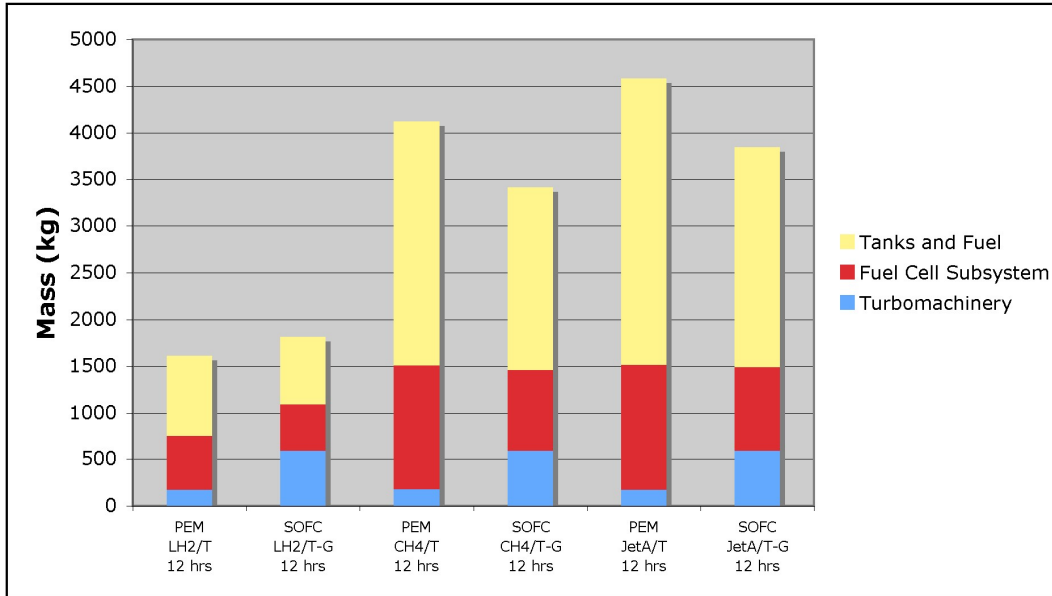
Figure 12.—Mass breakdown for select 1000 kW PEM and SOFC systems—12 hr endurance.
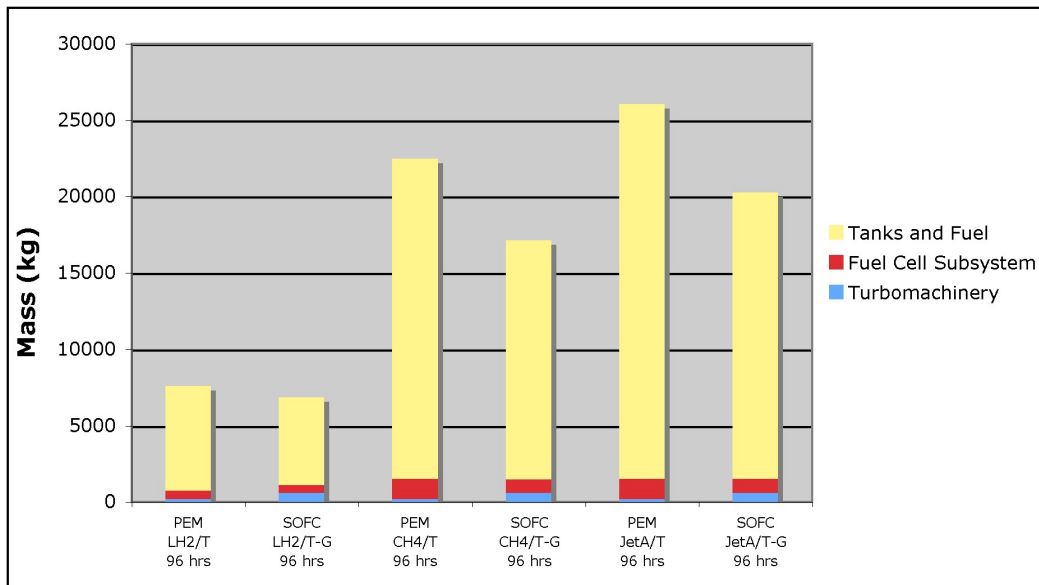
Figure 13.—Mass breakdown for select 1000 kW PEM and SOFC systems—96 hr endurance.

Figure 14 shows a comparison of total system mass as a function of mission duration for the same 10 kW PEM and SOFC systems. For a given fuel, the PEM systems start out lighter than the SOFC system, but eventually end up heavier with the crossover point moving toward lower mission durations for the heavier fuels. As was seen in the mass breakdown charts, at the lower mission durations the system mass is dominated by the hardware (fuel cell and turbomachinery). Although the PEM fuel cell subsystem mass is greater than the SOFC mass due to the more complex reformation and additional ancillaries, the overall SOFC hardware mass is greater due to the increased turbomachinery mass. As the mission duration increases and the tank mass becomes more dominant, the SOFC systems become lighter than the PEM systems due to the lower specific fuel consumption and, therefore, lower tank mass. In addition, for methane and Jet-A fuels, the SOFC hybrid systems benefit from increased energy efficiency

due to thermal integration. In the SOFC system, the hot reformate stream can be fed directly into the fuel cell whereas it must be significantly cooled before entering the PEM fuel cell. Also, since the SOFC waste heat is carried out by the air stream, it can be used to preheat the incoming air and fuel streams rather than being rejected via a radiator as in the PEM system.

Figure 15 shows the relative comparison of the corresponding tank volumes for these systems. The SOFC systems show a distinct advantage over PEM, especially as mission duration increases. Also, the Jet-A systems show the lowest volume due to the higher fuel density. The corresponding charts for the 100 and 1000 kW systems are included in the Appendix (figs. A11 to A14).

A trade study was conducted to examine the effect of increasing the efficiency of the PEM fuel cell stack by operating at a higher cell voltage (i.e. lower current density). Operating at a higher efficiency will lead to an increase in fuel cell stack mass, a decrease in fuel consumption and, therefore, fuel and tank mass, and a decrease in turbomachinery mass due to the lower air flow rates. For the purposes of this trade, the liquid hydrogen-fueled PEM-turbine configuration was chosen (fig. 3) since this system was found to be the lightest and most volume efficient of all of the hydrogen PEM systems studied. While this trade was conducted using hydrogen fuel, similar results should be seen for the methane and Jet-A systems as well. The operating point of the fuel cell was chosen as 150 mA/cm^2 and 0.85 V/cell. All other operational parameters and assumptions are the same as shown in table 2.
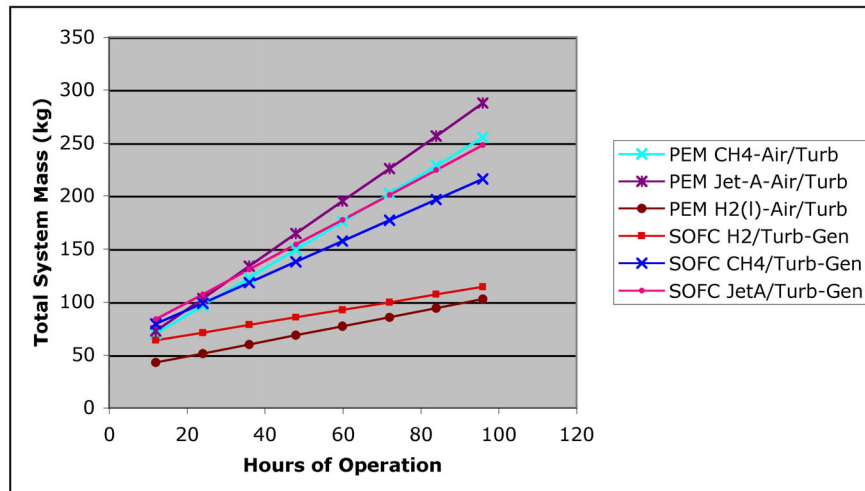
Figure 14.—System mass comparison of PEM and SOFC systems—10 kW net power output.
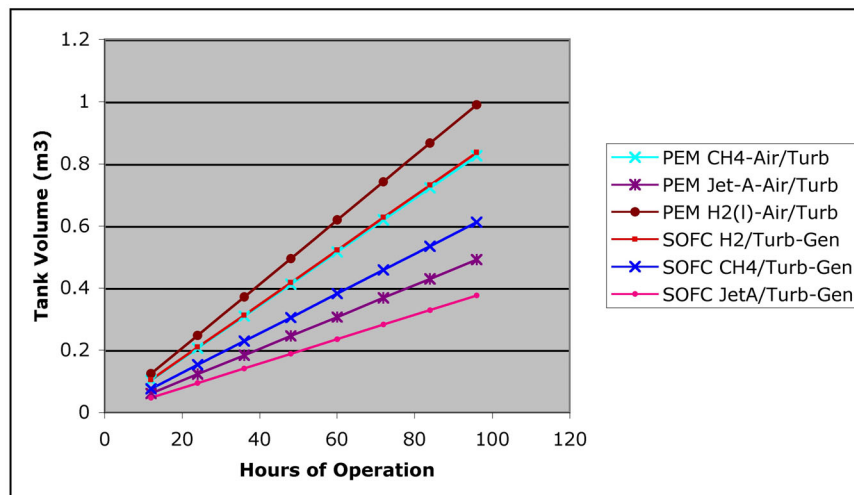
Figure 15.—Tank volume comparison for PEM and SOFC system—10 kW net power output.
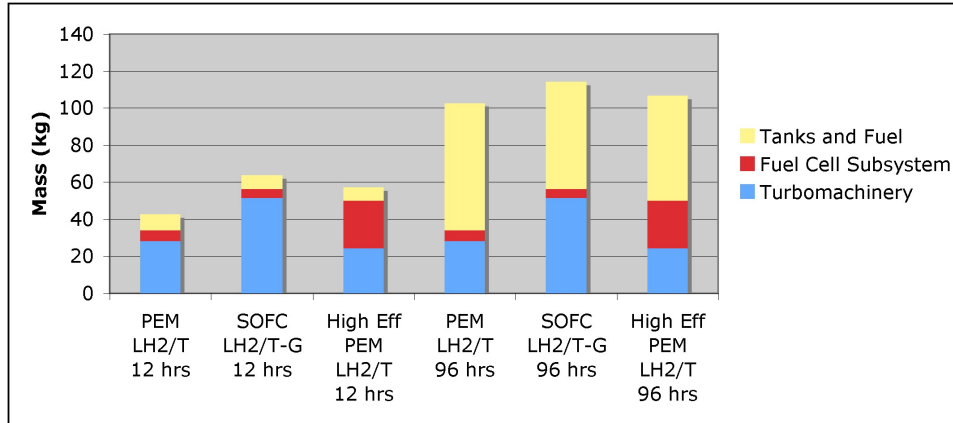
Figure 16.—Mass breakdown of 10 kW hydrogen-fueled systems
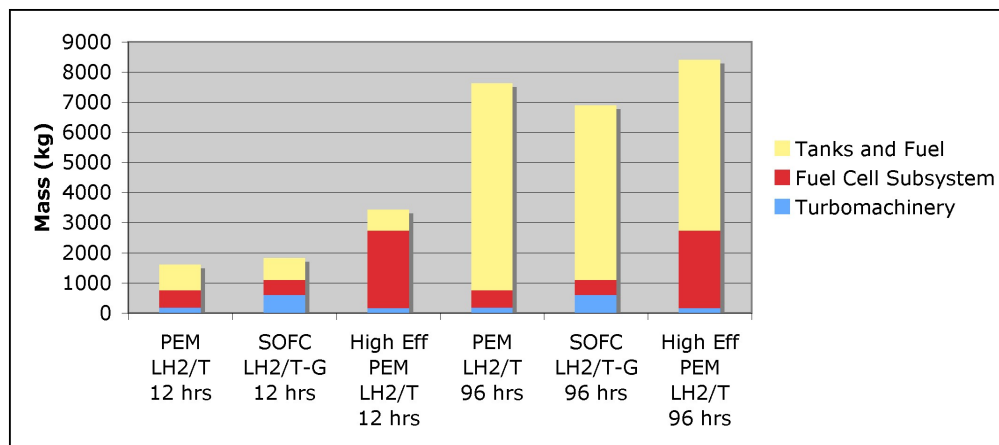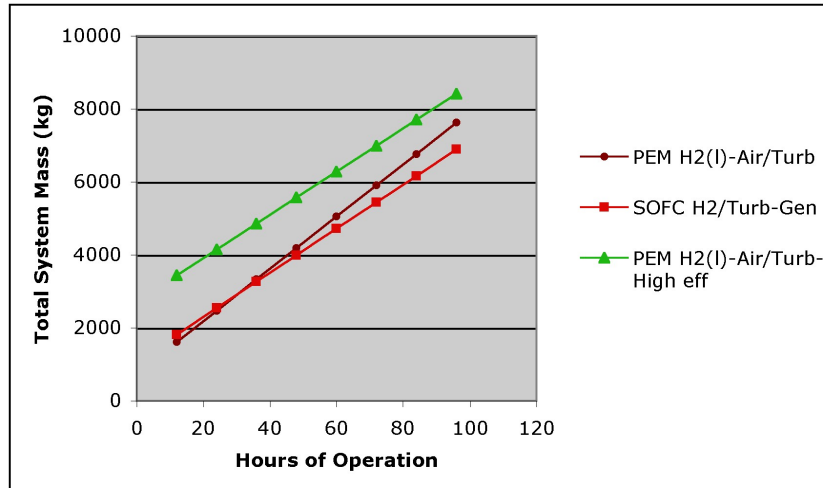including high efficiency—PEM for 12 and 96 hr endurance.
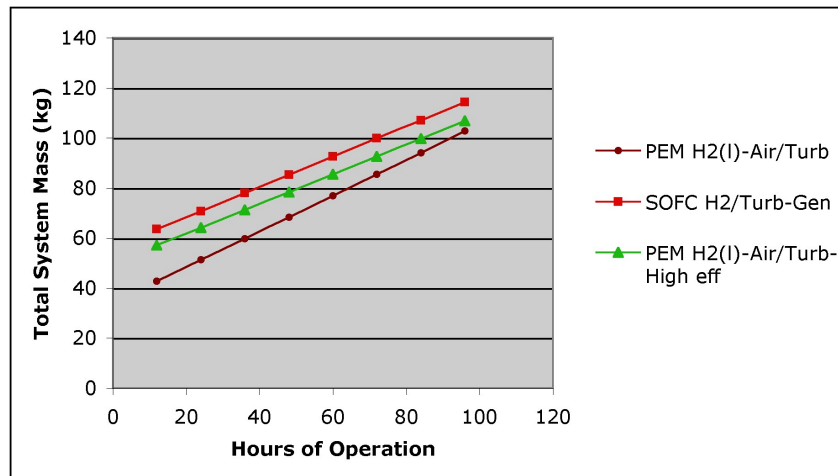
Figure 17.—System mass comparison of H₂-fueled systems including
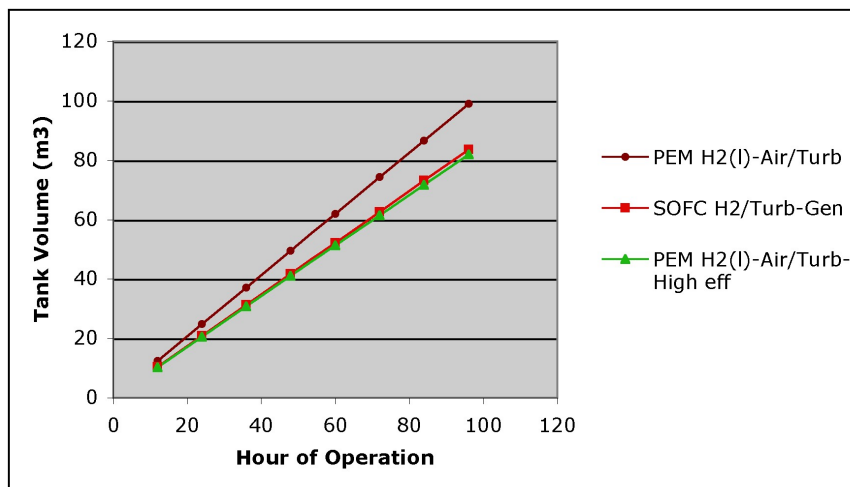high efficiency PEM—10 kW net power output.

Figure 16 shows the mass breakdown of the 10 kW, high efficiency PEM system as compared to the lower efficiency PEM system and the hydrogen-fueled SOFC hybrid system for mission durations of 12 and 96 hr. When compared to the lower efficiency PEM system at 12 hr, the high efficiency system shows a decrease in tank and fuel mass and turbomachinery mass due to the lower specific fuel consumption (0.053 kg/kW-hr vs. 0.064 kg/kW-hr). However, the increase in fuel cell mass results in the total system mass being greater for the high efficiency system. Yet, as mission duration increases and the tank and fuel mass becomes more dominant, the mass of the lower efficiency system approaches that of the high efficiency system and eventually surpasses it. This can be seen more clearly in figure 17, which shows the total system mass as a function of mission duration. By comparison, the SOFC system is slightly heavier than the high efficiency PEM system. As can be seen in figure 17, the lines are parallel, maintaining the same difference in mass as mission duration increases. This is due to the specific fuel consumptions of these two systems being nearly identical (0.053 kg/kW-hr for the high efficiency PEM vs. 0.054 for the SOFC hybrid). While the fuel cell subsystem and turbomachinery masses remain constant as mission duration increases, the tank and reactant mass of each of these systems increases at the same rate.

The tank volume comparison for the 10 kW systems is shown in figure 18. The high efficiency PEM system has a similar tank volume to the SOFC system since the specific fuel consumption is the same for

both systems. As expected, the high efficiency PEM shows a savings in tank volume over the lower efficiency PEM system.

Figure 19 shows the corresponding mass breakdown of the 1000 kW hydrogen-fueled systems for mission durations of 12 and 96 hr. As was previously discussed, the fuel cell subsystem becomes a greater fraction of the total mass than the turbomachinery as the power level increases due to the way in which each scales with power. This is especially significant for the high efficiency PEM system. At a 12 hr mission duration, the majority of the mass is carried in the fuel cell subsystem and results in this system weighing approximately twice that of the lower efficiency PEM system. At 96 hr, the disparity between the two systems is less with the high efficiency system only 10% heavier than the lower efficiency system. As mission duration increases further, the benefit of lower specific fuel consumption will eventually result in a lower mass for the high efficiency system. This is shown in figure 20. It is interesting to note that, unlike the 10 kW systems, the total mass of the high efficiency PEM system is greater than the SOFC hybrid system at the higher power levels due to the mass of the fuel cell subsystem with respect to the total system mass. The tank volume as a function of mission duration follows the same trend as the 10 kW systems and is shown in figure 21. The total mass and tank volume comparisons and mass breakdown chart for the 100 kW systems are contained in the Appendix (figs. A15 to A17).
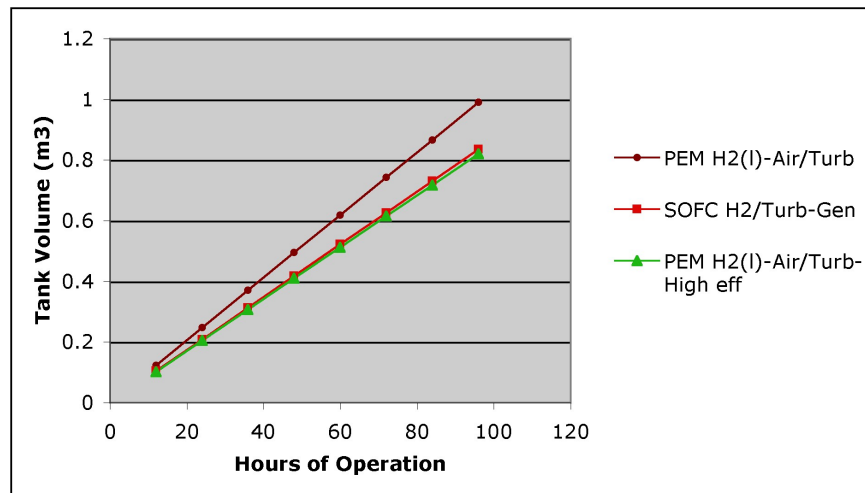
Figure 18.—Tank volume comparison of H_2-fueled systems including high efficiency PEM—10 kW net power output.

Figure 19.—Mass breakdown of 1000 kW hydrogen-fueled systems including high efficiency PEM for 12 and 96 hr endurance.

Figure 20.—System mass comparison of H_2-fueled systems including high efficiency PEM—1000 kW net power output.

Figure 21.—Tank volume comparison of H_2-fueled systems including high efficiency PEM—1000 kW net power output.

Conclusions

A variety of PEM- and SOFC-based power system architectures using hydrogen, methane, and Jet-A fuels were compared on a system mass and tank volume basis. For the PEM-based systems, the LH_2-fueled systems exhibit the lowest total system mass, but the highest tank volume due to the low storage density of hydrogen. Conversely, the Jet-A system exhibits the lowest tank volume and may be a better fuel choice for a volume-limited UAV. Coupling a turbine with the PEM fuel cell to run the compressors further reduces the system mass and tank volume by reducing the fuel cell power output and lowering the fuel flow rate. The SOFC- based systems benefit from the ability to recover the energy of the high temperature fuel cell exhaust streams in a hybrid configuration. Adding a generator to the system to offload some of the payload power from the fuel cell results in a reduction in overall system mass and tank volume. As mission duration and power output increase, the tanks tend to become a greater fraction of the total mass. For these cases, the SOFC hybrid systems offer an advantage over the PEM-based systems due to their lower specific fuel consumption. High efficiency operation of the PEM system increases fuel cell subsystem mass, but results in a lower total system mass than a PEM system run at lower efficiency for long mission durations.

Appendix
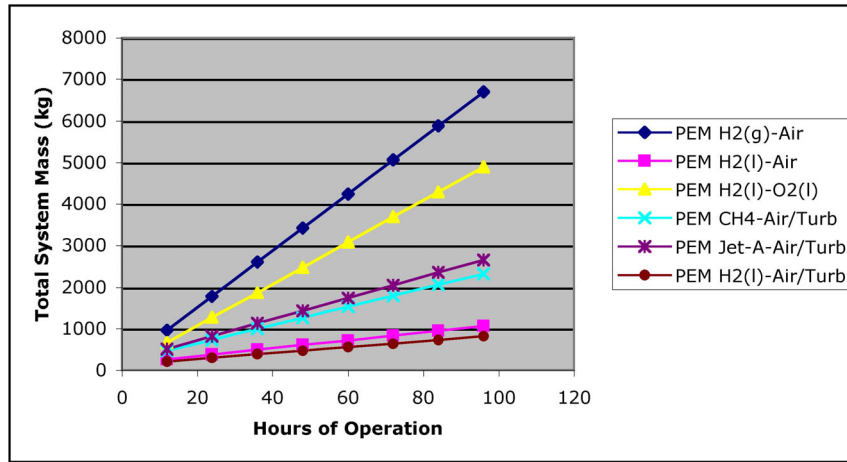
Figure A1.—PEM system mass summary—100 kW net output power.
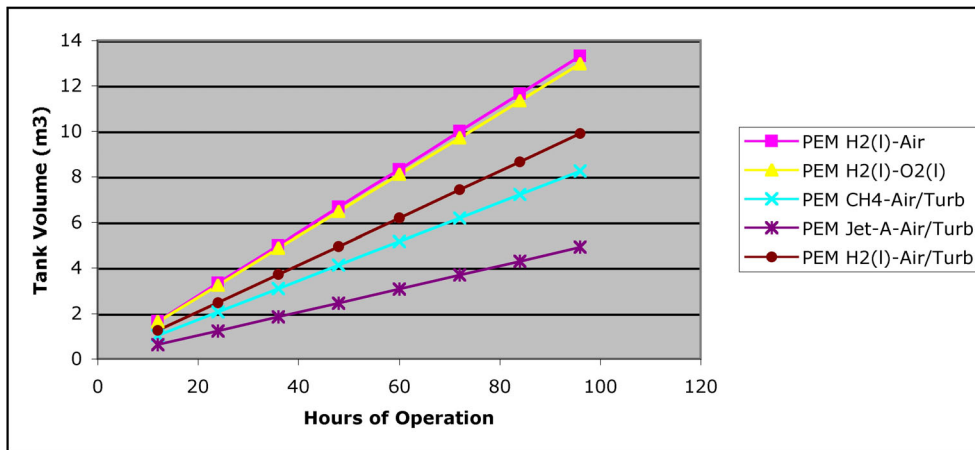
Figure A2.—PEM tank volume summary—100 kW net output power.
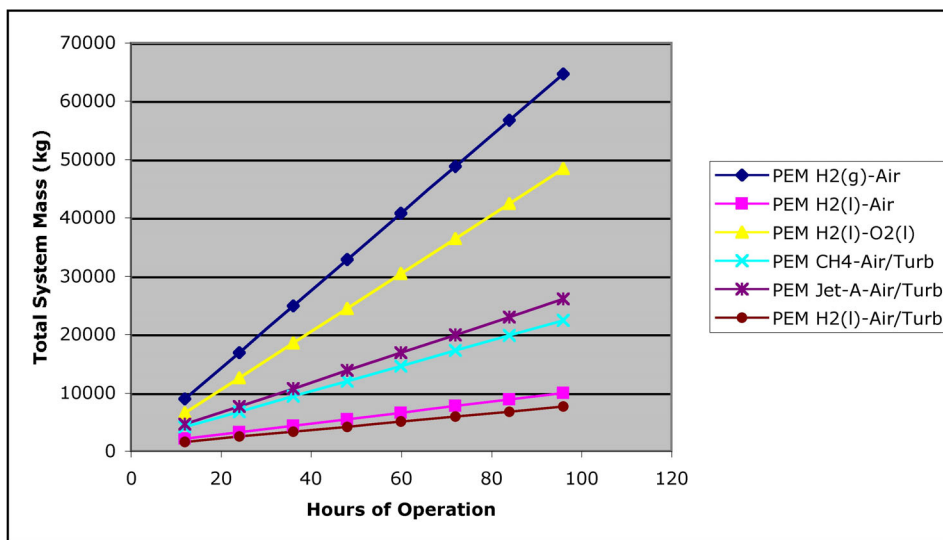
Figure A3.—PEM system mass summary—1000 kW net output power.
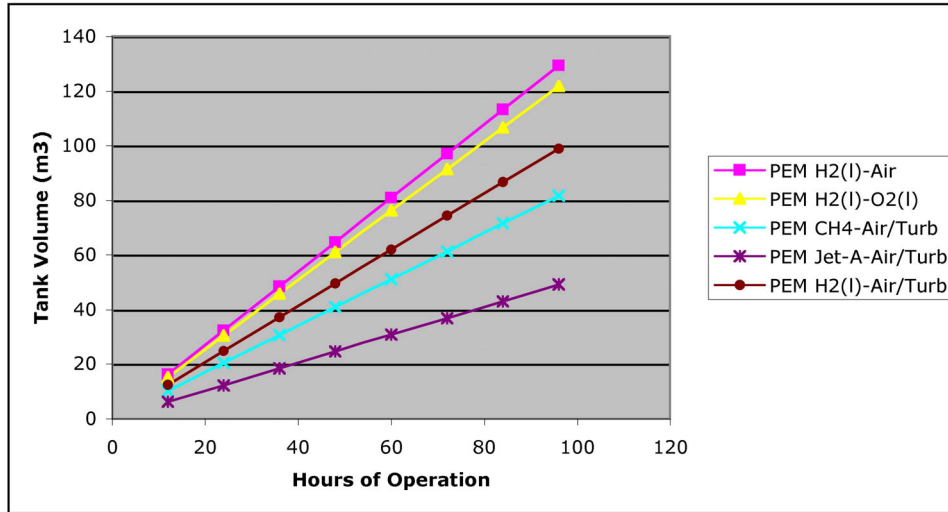
Figure A4.—PEM tank volume summary—1000 kW net output power.
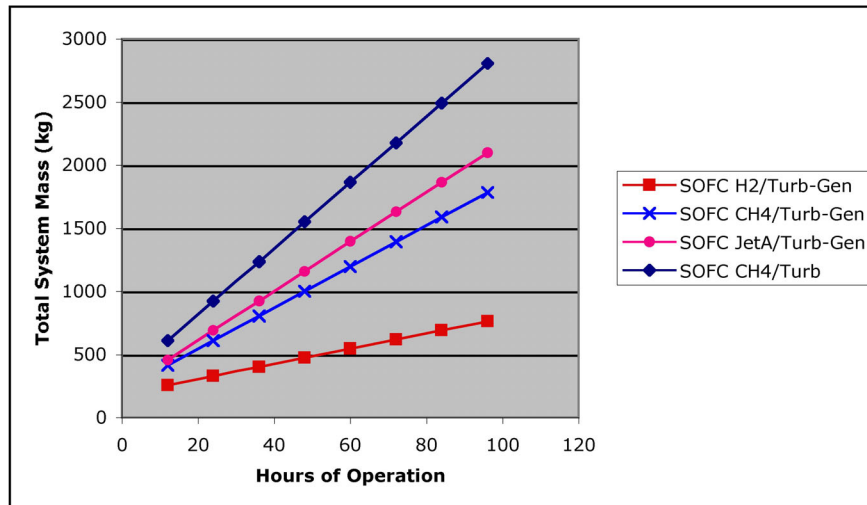
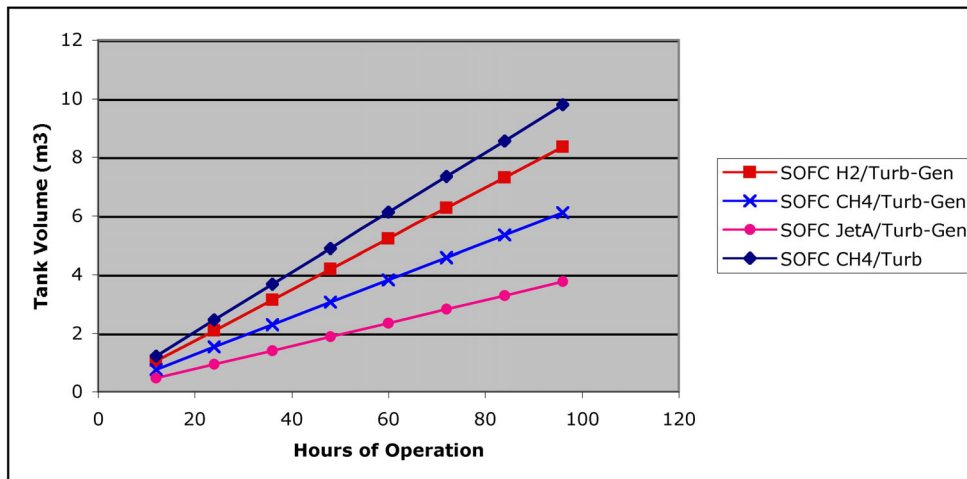Figure A5.—SOFC system mass summary—100 kW net output power.

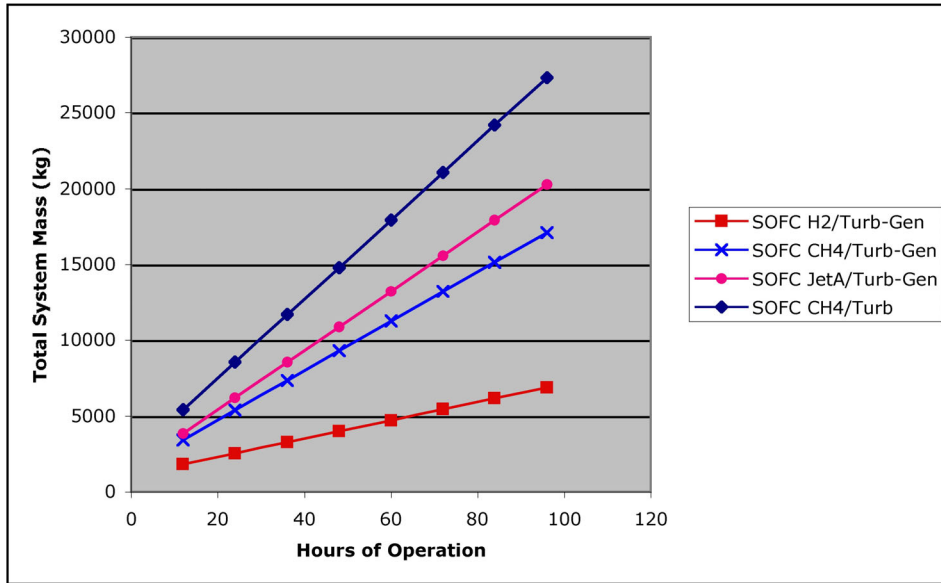Figure A6.—SOFC tank volume summary—100 kW net output power.

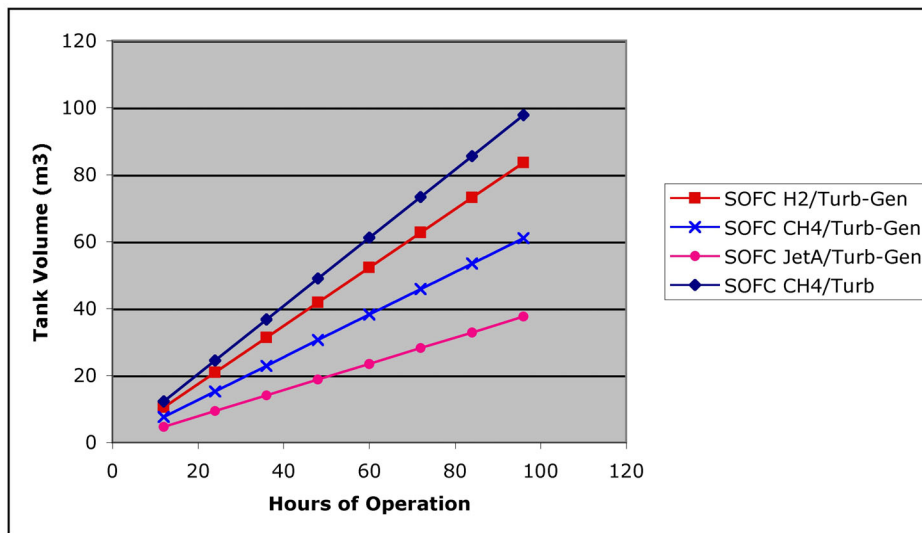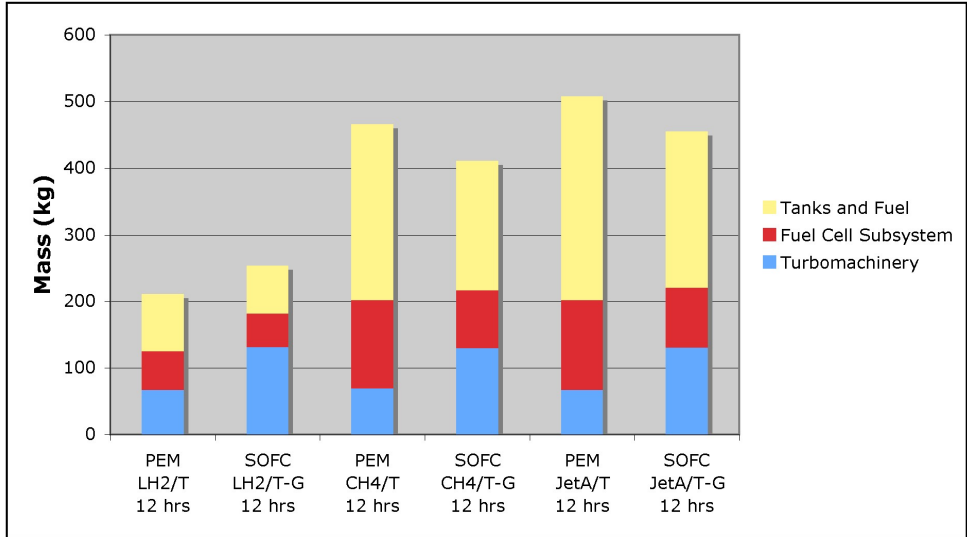Figure A7.— SOFC system mass summary—1000 kW net output power.

Figure A8.—SOFC tank volume summary—1000 kW net output power.

Figure A9.—Mass breakdown for select 100 kW PEM and SOFC systems—12 hr endurance.
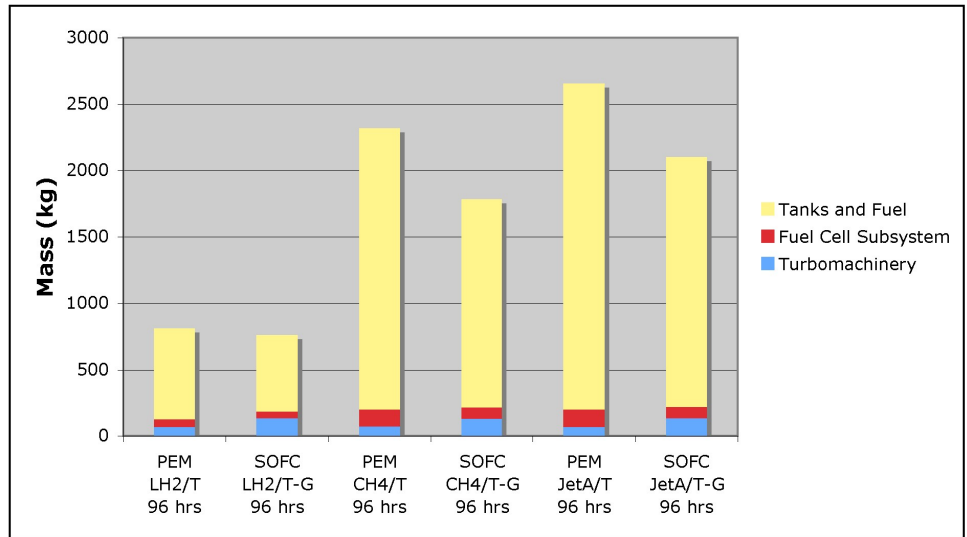
Figure A10.—Mass breakdown for select 100 kW PEM and SOFC systems—96 hr endurance.
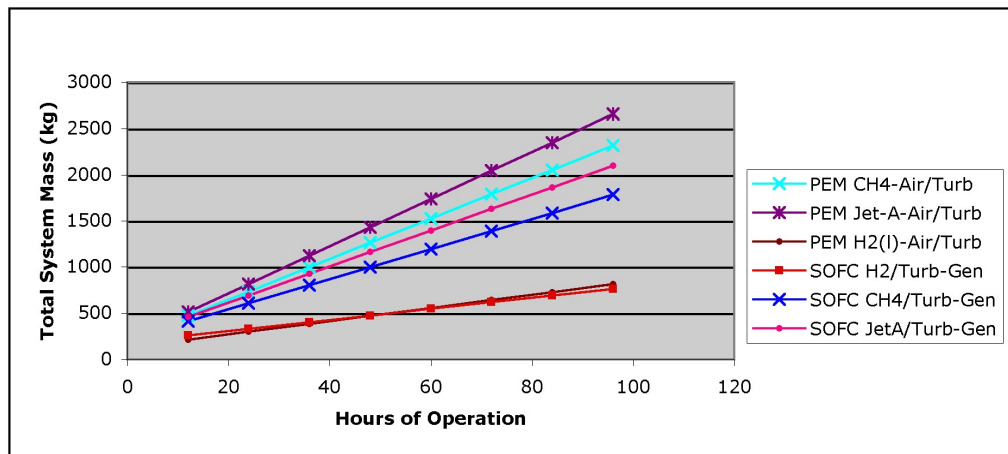
Figure A11.—System mass comparison of PEM and SOFC systems—100 kW net power output.
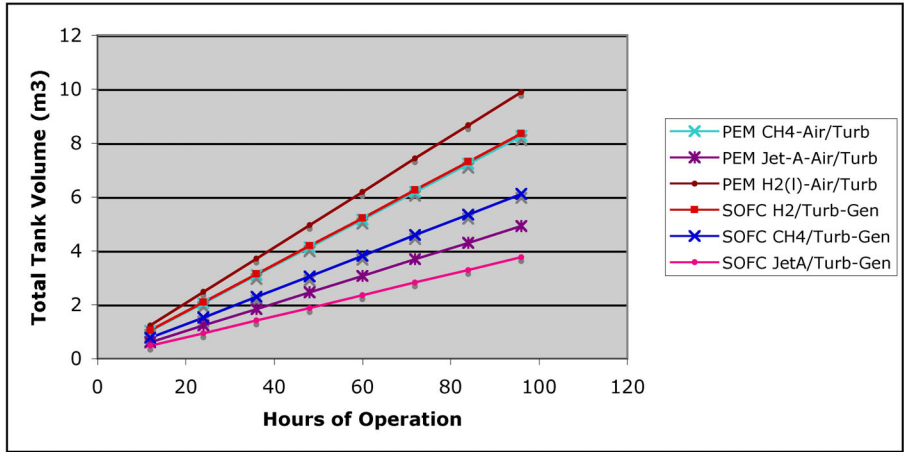
Figure A12.—Tank volume comparison for PEM and
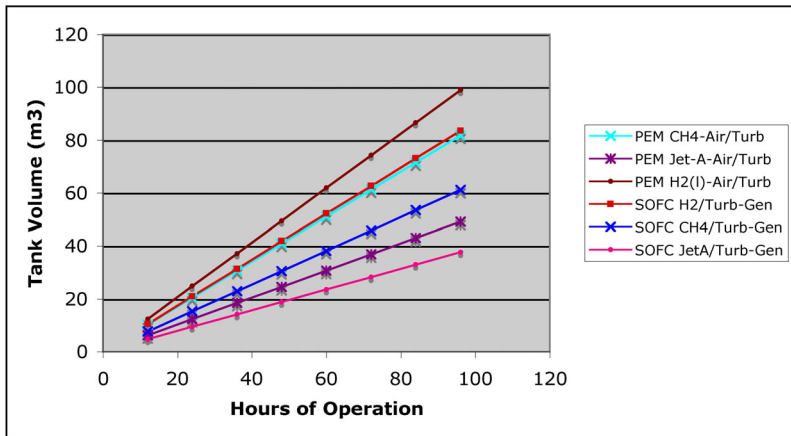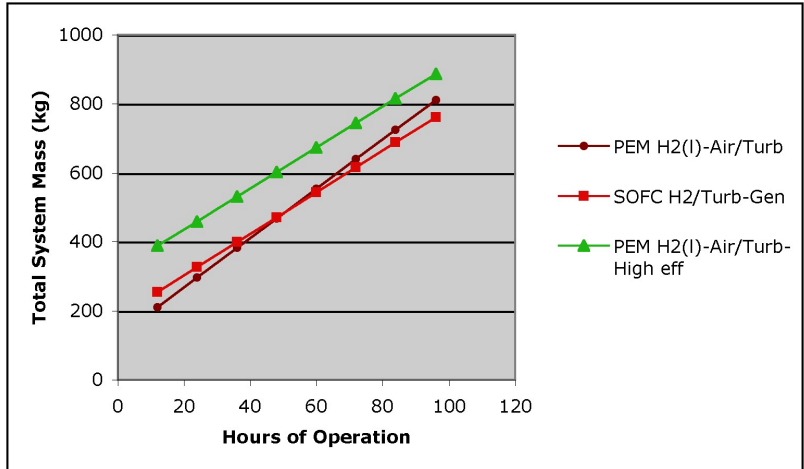SOFC system—100 kW net power output.
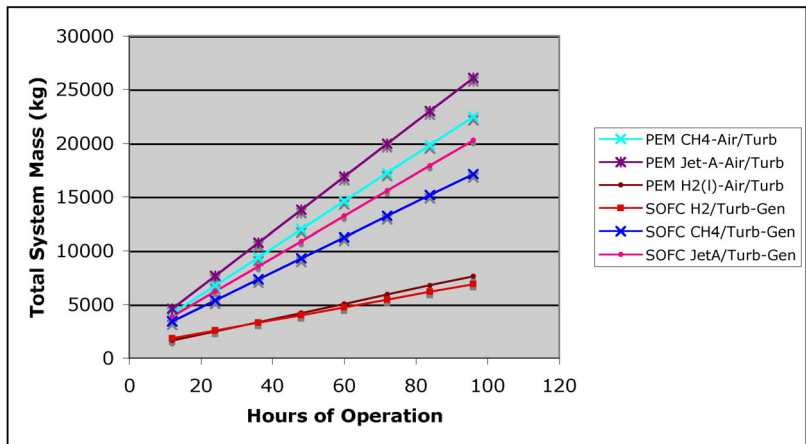
Figure A13.—System mass comparison of PEM and
SOFC systems—1000 kW net power output.

Figure A14—Tank volume comparison for PEM and
SOFC system—1000 kW net power output.

Figure A15.—System mass comparison of H_2-fueled systems including high efficiency PEM—100 kW net power output.
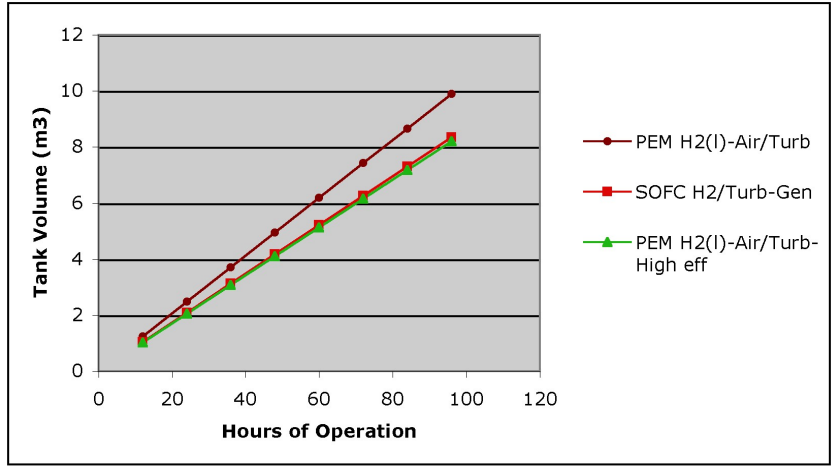

Figure A16.—Tank volume comparison of H_2-fueled systems including high efficiency PEM—100 kW net power output.
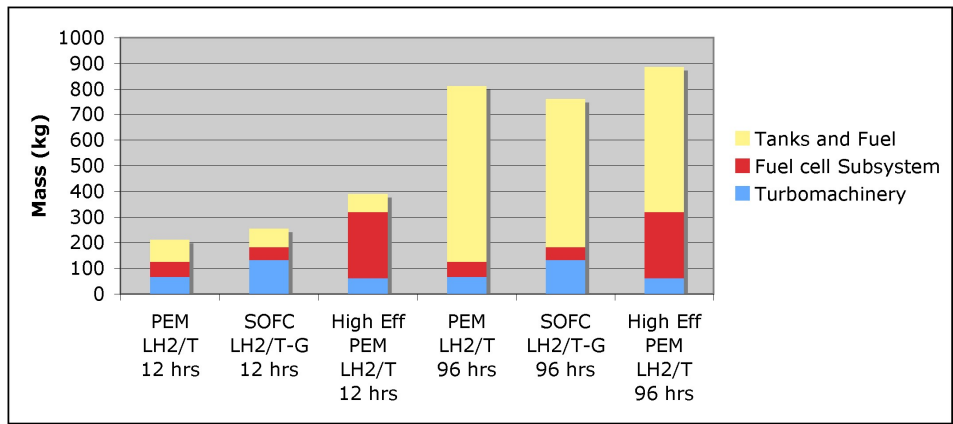

Figure A17.—Mass breakdown of 100 kW hydrogen-fueled systems including high efficiency PEM for 12 and 96 hr endurance.

References

1. J. Larmine and A. Dicks, *Fuel Cell Systems Explained*, John Wiley & Sons, Ltd., 2000.
2. E. Achenbach, "International Energy Agency- Annex II, Modeling and Evaluation of Advanced SOFC, Subtask A: Numerical Modeling, Experimental Data Base and Validation, Activity A2, Stack Modeling," 31 Mar. 1996.
3. S. Gordon and B. McBride, "Computer Program for Calculation of Complex Chemical Equilibrium Compositions and Applications," NASA Reference Publication 1311, Oct. 1994.
4. A. Glassman, "Computer Code for Preliminary Sizing Analysis of Axial-Flow Turbines," NASA CR–4430, 1992.
5. A. Glassman, "Modeling Improvements and Users Manual for Axial-Flow Turbine Off-Design Computer Code AXOD," NASA CR–195370, Aug.1994.
6. J. Gillis, "Users Manual for the LACEX Cryo-To-Air Heat Exchanger Design Code," NASA Lewis Research Center, Mar. 1988.
7. "Helios Energy Storage System Technical Review," Presentation by AeroVironment, Inc., Sept. 2000.
8. G. Daniel Brewer, Hydrogen Aircraft Technology, CRC Press, 2001.
9. Interstate Products, Inc. website, http://www.interstateproducts.com/pillow_tanks.htm.
10. Dupont Fuel Cell- Dupont Membrane Electrode Assemblies (MEA3, MEA5, MEA7), Dupont Product information Sheet (DFC201), Feb 2004.
11. General Motors Corp., "General Motors Introduces World's Most Powerful Fuel cell Stack," Press Release, Sept. 2001.

1. REPORT DATE (DD-MM-YYYY) 09-05-2007	2. REPORT TYPE Technical Memorandum	3. DATES COVERED (From - To)

4. TITLE AND SUBTITLE
An Analysis of Fuel Cell Options for an All-Electric Unmanned Aerial Vehicle

5a. CONTRACT NUMBER

5b. GRANT NUMBER

5c. PROGRAM ELEMENT NUMBER

6. AUTHOR(S)
Kohout, Lisa, L.; Schmitz, Paul, C.

5d. PROJECT NUMBER

5e. TASK NUMBER

5f. WORK UNIT NUMBER
WBS 561581.02.08.03.06.01

7. PERFORMING ORGANIZATION NAME(S) AND ADDRESS(ES)
National Aeronautics and Space Administration
John H. Glenn Research Center at Lewis Field
Cleveland, Ohio 44135-3191

8. PERFORMING ORGANIZATION REPORT NUMBER
E-15900

9. SPONSORING/MONITORING AGENCY NAME(S) AND ADDRESS(ES)
National Aeronautics and Space Administration
Washington, DC 20546-0001

10. SPONSORING/MONITORS ACRONYM(S)
NASA

11. SPONSORING/MONITORING REPORT NUMBER
NASA/TM-2007-214699

12. DISTRIBUTION/AVAILABILITY STATEMENT
Unclassified-Unlimited
Subject Category: 07
Available electronically at http://gltrs.grc.nasa.gov
This publication is available from the NASA Center for AeroSpace Information, 301-621-0390

13. SUPPLEMENTARY NOTES

14. ABSTRACT
A study was conducted to assess the performance characteristics of both PEM and SOFC-based fuel cell systems for an all-electric high altitude, long endurance Unmanned Aerial Vehicle (UAV). Primary and hybrid systems were considered. Fuel options include methane, hydrogen, and jet fuel. Excel-based models were used to calculate component mass as a function of power level and mission duration. Total system mass and stored volume as a function of mission duration for an aircraft operating at 65 kft altitude were determined and compared.

15. SUBJECT TERMS
Fuel cells; Hydrogen; Hydrocarbon fuels; Proton exchange membrane fuel cells; Solid oxide fuel cells

16. SECURITY CLASSIFICATION OF:			17. LIMITATION OF ABSTRACT	18. NUMBER OF PAGES	19a. NAME OF RESPONSIBLE PERSON Lisa L. Kohout
a. REPORT U	b. ABSTRACT U	c. THIS PAGE U		29	19b. TELEPHONE NUMBER (include area code) 216-433-8004

Standard Form 298 (Rev. 8-98)
Prescribed by ANSI Std. Z39-18